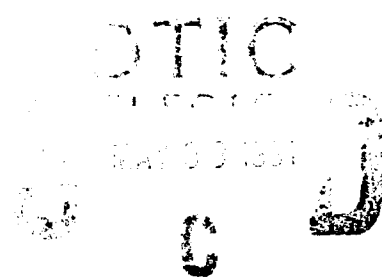AD-A235 675

Noncontact
Small-Diameter-Bore Gauge

M. A. Lind
R. F. Johnson

QUEST Integrated, Inc.
21414 - 68th Avenue South
Kent, Washington 98032
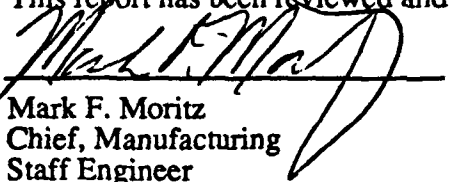(206) 872-9500

October 1990

Prepared for

Ballistic Missile Organization/SSD
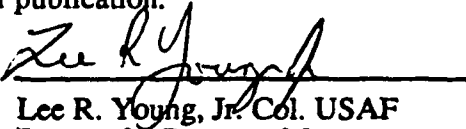Norton Air Force Base, California 92409-6468

Mark F. Moritz
Chief, Manufacturing
Staff Engineer
For Program Management

Lee R. Young, Jr. Col. USAF
Deputy for Program Management

REPORT DOCUMENTATION PAGE

Public reporting burden for this collection of information is estimated to average 1 hour per response, including the time for reviewing instructions, searching existing data sources, gathering and maintaining the data needed, and completing and reviewing the collection of information. Send comments regarding this burden estimate or any other aspect of this collection of information, including suggestions for reducing this burden, to Washington Headquarters Services, Directorate for Information Operations and Reports, 1215 Jefferson Davis Highway, Suite 1204, Arlington, VA 22202-4302, and to the Office of Management and Budget, Paperwork Reduction Project (0704-0188) Washington, DC 20503

1. AGENCY USE ONLY (Leave blank)	2. REPORT DATE October 1990	3. REPORT TYPE AND DATES COVERED Final; 31 May 90 – 13 Nov 90

4. TITLE AND SUBTITLE Noncontact Small-Diameter-Bore Gauge	5. FUNDING NUMBERS F04704-90-C-0033

6. AUTHOR(S)

M. A. Lind and R. F. Johnson

7. PERFORMING ORGANIZATION NAME(S) AND ADDRESS(ES) Quest Integrated, Inc. 21414 - 68th Avenue South Kent, WA 98032	8. PERFORMING ORGANIZATION REPORT NUMBER BMO-TR-90-127

9. SPONSORING/MONITORING AGENCY NAME(S) AND ADDRESS(ES) Ballistic Missile Organization/SSD Norton AFB, CA 92409-6468	10. SPONSORING/MONITORING AGENCY REPORT NUMBER

11. SUPPLEMENTARY NOTES

12a. DISTRIBUTION/AVAILABILITY STATEMENT Approved for public release; distribution is unlimited.	12b. DISTRIBUTION CODE

13. ABSTRACT (Maximum 200 words)

Current Peacekeeper and small ICBM guidance systems require measurement tolerances of 5 microinches on bores used in critical bearings in the SFIR (Specific Force Integrating Receiver) and TGG (Third Generation Gyro). Quest Integrated, Inc., conducted a Phase I program to investigate the feasibility of developing a noncontact measurement system based on the principle of optical triangulation for characterizing the diameter and cylindricity of these bores. The study showed that the fundamental limitations to the measurement technique are in the sub-microinch range. A first prototype probe was constructed and used to demonstrate the measurement of internal diameters to the resolution limit of the A/D converters employed (8 microinches). Once developed, the proposed probe will allow easy measurement of the internal dimensions of cylindrical shapes. This tool would have wide applications as a generic precision measuring tool.

14. SUBJECT TERMS Bore diameter, Cylinder, Internal dimensions, Laser, Optical triangulation, Precision measurement	15. NUMBER OF PAGES 30
	16. PRICE CODE

17. SECURITY CLASSIFICATION OF REPORT Unclassified	18. SECURITY CLASSIFICATION OF THIS PAGE Unclassified	19. SECURITY CLASSIFICATION OF ABSTRACT Unclassified	20. LIMITATION OF ABSTRACT UL

NSN 7540-01-280-5500

ACKNOWLEDGEMENTS

DTIC
COPY
INSPECTED
6

Accession For
NTIS GRA&I
DTIC TAB
Unannounced
Justification

By
Distribution/
Availability
Dist
A-1

TABLE OF CONTENTS

LIST OF FIGURES

INTRODUCTION

Description of the Problem

Current Peacekeeper and small ICBM guidance systems require tolerances of 5 microinches (125 nm) on precision bearing bores used on the SFIR (Specific Force Integrating Receiver) and TGG (Third Generation Gyro). Currently, these bores are inspected using a manually loaded air gauge. It is possible for the operator to damage these pyroceram bores while attempting to measure them. The part must then be reworked or scrapped. The development of a mechanically loaded, highly accurate, noncontact measurement system for small-diameter bores is desired, since it could save many man-hours and reduce the scrap rate on very expensive parts.

The parts requiring these high-accuracy measurements are cylinders approximately 0.5 inch long with an outside diameter of approximately 0.5 inch. They have a concentric inner bore approximately 0.25 inch in diameter. The specified rms surface finish of the parts varies between 2 and 8 microinches, depending upon the point in the manufacturing process. The high-quality surface finish of the pyroceram material used for the parts leaves the surfaces to be measured highly reflective and highly specular (mirror-like).

The objective of this program was to demonstrate the feasibility of providing a relatively low cost, temperature-stable, noncontact caliper-based tool that can be applied to the measurement of the diameter and cylindricity (circularity, straightness, and taper) of the above parts. A longer term objective of the program is to be able to expand the capabilities of the tool to include the measurement of flatness, parallelism, and perpendicularity of the surfaces surrounding the bore as well as true position of the bore with respect to the overall diameter and external cylindricity of the part.

Phase I Feasibility Study

The most often discussed noncontact measurement systems used over the dimensional ranges of interest are based on heterodyne laser interferometry. While such measurement systems are technically feasible for the required application, the cost and complexity of these systems are relatively high. The approach taken by Quest Integrated, Inc., in this Phase I feasibility study was to investigate the possibility of developing a high-accuracy noncontact measuring system based on the principle of optical triangulation.

This final report presents the measurement approach and describes the operational caveats and sources of error for the selected approach. It then discusses the methodology employed in fabricating the laboratory prototype probe and describes the experimental results obtained on the resolution, repeatability, and overall accuracy of the probe. Finally, it presents recommendations for a Phase II program leading to a low-cost measurement tool for accurately characterizing the diameter and cylindricity of bored holes and other tubular structures to better than 1 microinch.

The Phase II program will involve the finalizing of the design and the manufacture, testing, and validation of a full-function prototype measuring system. The potential advantages to the proposed optical triangulation bore measurement gauges are low cost, rugged construction, and ease of use.

BACKGROUND

General Approach

Optical triangulation has been used in various forms for many centuries to determine the distance or range of an object from an observer. The fundamental concept used in the proposed measurement tool is illustrated in Figure 1 below. An object, or in our case a surface, is illuminated by a source with a known geometry. The light reflected from the surface is imaged onto a position-sensitive detector as illustrated. As the source/detector is displaced from the surface, the position of the image of the illuminated surface spot changes on the detector. Using appropriately designed imaging optics, the magnitude of the position change on the detector can be directly related to the distance from the source/detector to the surface.
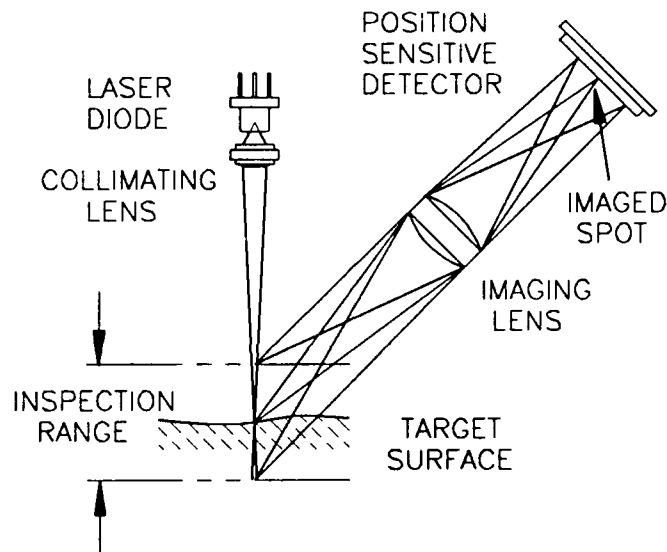
Figure 1. Optical Triangulation for Distance Measurements

The principles underlying laser-based optical triangulation profilometry of surfaces are well established and in use in many types of instrumentation today. Typical measurement accuracies for commercial distance-measurement devices are in the 100 to 1000 microinch range. These devices are packaged in a variety of formats as small as 0.5 inch in diameter.

The challenge of this program was to package a device that can measure the distance between two opposing surfaces in bores as small as 0.25 inch in diameter with accuracies 2 to 3 orders of magnitude greater than the commercial devices. Accuracies in the required range require careful attention both to the fundamental limitations of the electro-optic devices employed and to the influence of environmental parameters, particularly temperature.

The approach adopted for the feasibility experiments was to build a temperature-stable optical triangulation probe capable of measuring the relative distance between two parallel

opposing surfaces with a relative resolution exceeding 1 microinch. The intent of the program was to demonstrate this caliper diameter measurement as the first step in measuring multiple diameters to characterize the interior of high-reflectivity specular bores.

Theory of Operation

Figure 2 illustrates two practical implementations of the optical triangulation technique to the measurement of relative surface displacement. In the first case, the light source is a focused or narrowly collimated laser diode. The output of the diode is projected onto a diffuse surface. An image of the spot intercepting the surface is formed on a linear position detector by the imaging lens. As the surface displacement changes, the image is translated on the linear position detector.
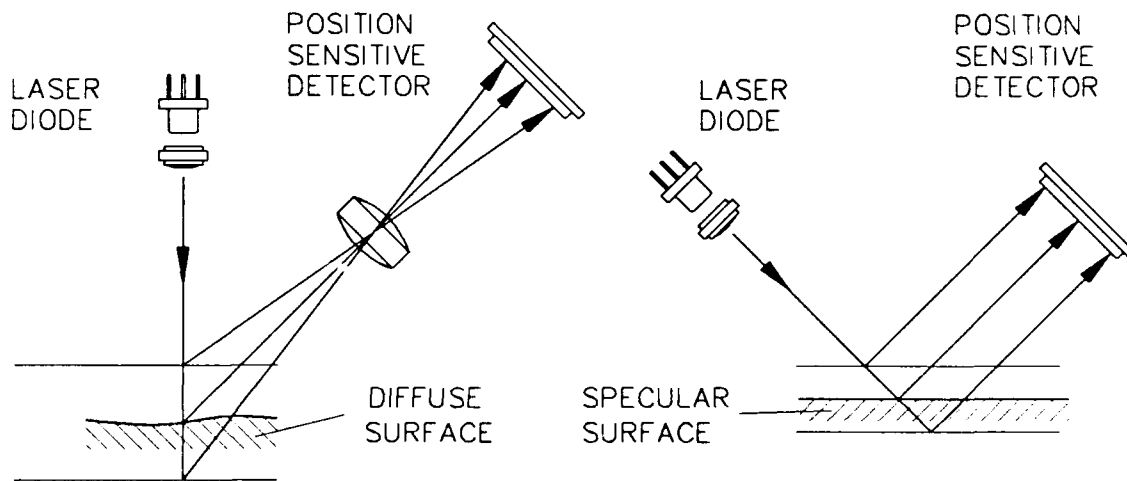
Figure 2. Physical Implementation of Diffuse and Specular Optical Triangulation Measurements

Also illustrated is an implementation for a specular surface. Here the laser beam is reflected directly off the target surface onto the linear position detector. This specular reflection technique only works for surfaces that exhibit a highly specular reflectance. Notice that the imaging lens is not needed in this application. This specular technique was chosen for implementation in the feasibility demonstration because of the simplicity of the optical path and the specular finish of the bore surfaces to be measured.

Operation of the linear position or lateral-effect photodiode is illustrated in Figure 3. The light striking the surface of the diode generates photocurrents at the two anodes of the device with respect to the cathode. The magnitude of the normalized difference of the two anode currents is proportional to the position of the centroid of the light spot. For most commercial detectors, this normalized signal is usually close to linear over the central 80% of the active area of the detector.

Calibrating this output signal from the detector for known distances from the detector/ source to the target provides an accurate and repeatable means of measuring the distance from the source/detector position to the illuminated surface. The resolution and

repeatability of the device depends only on the relative stability of the source/detector assembly and the noise generated by the source, the detector, and the analysis electronics.

ANODE 1

$$I_1$$

GENERATED PHOTOCURRENTS

IMAGED SPOT OF LIGHT

CATHODE

SILICON ELEMENT

$$\frac{I_1 - I_2}{I_1 + I_2} = \begin{array}{c} \text{NORMALIZED} \\ \text{OUTPUT} \end{array}$$

$$I_2$$

ANODE 2
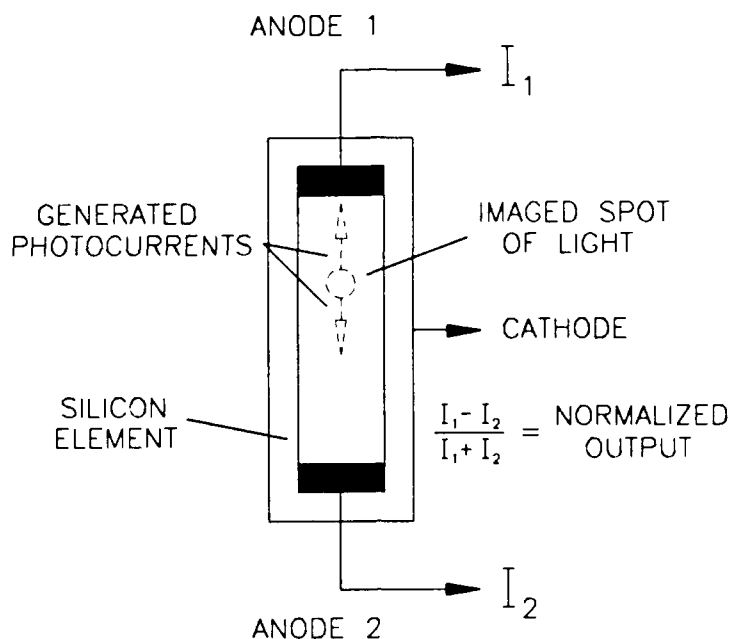
Figure 3. Lateral-Effect Photodetector

By employing multiple optical triangulation sensors in a single probe, simultaneous measurements can be made in various geometrical configurations. In particular, an interior caliper measurement requires the implementation of two back-to-back devices. The total characterization of an interior elliptical cylinder requires a minimum of two diameters (four radii), a rotation, and a translation.

This initial study was directed at determining the performance of a single diameter measure-ment probe. The expanded system for the complete measurement is described later in the report.

Practical Considerations

Numerous practical considerations are important in determining the feasibility and the fundamental limitations of a probe with the desired attributes. These are discussed briefly below.

Light Source Noise

Consider an optical source comprised of a laser diode coupled to a multimode optical fiber terminated by a quarter-pitch GRIN lens. This source provides a compact, easily directable, collimated, nearly monochromatic light beam that is nicely suited to the task at hand. However, both the amplitude stability and the geometrical stability in these components can cause systematic errors and random noise in the measurement.

For example, solid-state laser diodes are very attractive sources from the point of view of their small emittance geometry (high illuminance), narrow bandwidth spectral distribution, and compact size. However, these lasers do have some serious drawbacks for precision measurements. Because of the short cavity length, they tend to mode hop, especially at low output powers. The mode hopping, which is a fur tion of the junction temperature and input current, results in small changes in the output beam power distribution geometry. One of the requirements of the source in our application is the geometric stability of the beam centroid.

To mitigate the mode hopping problems the lasers must be feedback stabilized via their optical output power at relatively high output powers. It is nearly impossible to predict *a priori* the degree to which mode hopping will affect the measurement in the resolution range of interest. The expected effects manifest themselves as discontinuous jumps in the apparent measurement distance. If the source can be selected and controlled to yield jumps less than 1 microinch, then the design can be successful.

The throughput and the mode stability of the light source depend on the alignment of the optical components and the selection of the fiber. The coupling of the laser to the transmission fiber optic is a source of potential amplitude and geometrical error. A rigid, thermally stable connection is required. Stability of the GRIN collimating lens with respect to the fiber is still another source of error. The fibers must maintain a stable position to ensure stable pointing of the exit beam. The GRIN lenses must be cemented rigidly to the ends of the fibers.

Detector and Amplifier Noise

The electrical noise generated by the detector and the associated circuitry must be less than the required measurement accuracies for the bore gauge. The amount of noise generated determines the system bandwidth needed to achieve the necessary measurement accuracies. The more noise generated by the circuitry, the smaller the bandwidth and the longer it takes to make the measurement. If the bandwidth becomes too small, DC drift considerations become significant.

The detector/amplifier configuration chosen for the feasibility study is a standard transimpedance connection. The amplifier converts the current generated by the lateral cell to a voltage that can be read by a computer. The particular operational amplifier (op-amp) chosen for this application is the LT1012 by Linear Technology. It is a low-noise amplifier with particularly good DC characteristics. There are a number of noise sources in the detector/amplifier combination, and these are listed in Table 1.

The values for the first two noise sources in the table are listed in the data sheet for the op-amp and are typical for low-noise, FET input op-amps. The detector shot (or Schottky) noise comes from the photocurrent flowing in the detector and is calculated by the following equation:

$$\text{Detector Schottky Noise} = \sqrt{2 \, q \, I_D}$$

where $\quad q = 1.6 \times 10^{-19}$ coulombs

$\qquad I_D$ = detector current in amps

Table 1. Noise Source Summary

NOISE SOURCE	INPUT REFERRED NOISE	RMS NOISE AT OUTPUT OF AMPLIFIER (50-Hz Bandwidth)
Op-amp Voltage Noise	$\frac{17nV}{\sqrt{Hz}}$ (at 10 Hz)	6.8×10^{-6} volts
Op-amp Current Noise	$\frac{20 fA}{\sqrt{Hz}}$ (at 1C Hz)	2.1×10^{-9} volts
Detector Shot Noise	$\frac{17.9 pA}{\sqrt{Hz}}$ (at 1.0 mA)	2.4×10^{-6} volts
Detector Johnson Noise	$\frac{0.58 pA}{\sqrt{Hz}}$ (R_p = 48 kΩ)	61.5×10^{-9} volts
Amplifier Feedback Resistor Noise	$\frac{1 pA}{\sqrt{Hz}}$ (R_f = 15 kΩ)	0.11×10^{-6} volts
TOTAL NOISE		7.2×10^{-6} volts

The Schottky noise calculated from the above equation is in units of amps per square root of bandwidth. This noise source comes into play when there is a large incident light level on the detector, such as in this application.

The next noise source is the detector Johnson (or thermal) noise. Although present in all detectors, it is much larger in the lateral cell type of photodetector because of the bulk resistance media on the back of the detector. The final source is the Johnson noise from the feedback resistor connected between the output of the op-amp and the inverting input of the op-amp. This resistor sets the output voltage to the detector photocurrent gain of the detector/amplifier combination. For this application, the resistor was set to 15 kohms The equation for calculating the noise contributions from all thermal sources (Johnson noise) is:

$$\text{Noise Current} = \sqrt{\frac{4 k T}{R}}$$

where k = 1.33×10^{-23} joules/K
T = temperature in degrees Kelvin
R = resistance in ohms

The resulting noise current is in units of amps per square root of bandwidth.

The second column in Table 1 results from applying the two equations given above. The third column is the resulting rms noise as seen at the output of the amplifier after factoring in the 50-Hz bandwidth of the system. All noise sources except the op-amp voltage noise are subject to the 50-Hz bandwidth. The op-amp voltage noise, because of the particular amplifier topology, sees a much larger bandwidth and therefore is the largest noise contributor. The final system will have an additional stage of filtering to reduce this bandwidth to 50 Hz as well. Since each noise source is uncorrelated with the remaining sources, the total noise is the square root of the sum of squares of the individual noise sources.

The feasibility test probe has a sensitivity of approximately 50 microvolts per microinch. Comparing this value with the total rms noise output of 7.2 microvolts indicates that the noise from the detector or amplifier will not be a limiting factor in the system, particularly considering that the noise can easily be lowered to 2.4 microvolts rms by further reducing the bandwidth.

Geometrical Error

There are numerous sources of design-specific geometrical error that are possible with the proposed noncontact optical caliper measurement technique. Detector nonlinearity, tilt error, taper error, and concentricity error are discussed below for a probe with a 45-degree incident source beam configuration.

The linearity error of the detector (the output signal verses the position of the centroid of the light spot on the detector) is a large source of potential error. Typically, only the center 60% to 80% of the active area of the detector is specified by the detector manufacturer to be linear. In practice, Quest has found even this limited range to be optimistic. Fortunately, a simple calibration of the detectors can effectively eliminate this source of error. The calibration is performed by measuring a standard set of known displacements (or diameters) and recording the output signal(s). Since the output signals from a single detector are always monotonic, the output signal of each detector can be related to actual wall displacement via a look-up table. This process is illustrated in the experimental results below.

If the measurement probe is tilted within the opposing surfaces to be measured, then additional errors may occur depending on the specific geometry of the probe in relation to the surfaces being measured. In the case of measuring right circular cylinders, two types of error should be considered: ellipticity error and specular direction.

First consider the ellipticity error. Unless the measurement is performed perpendicular to the axis of the cylinder, the probe will measure an elongated dimension along the axis of tilt. The diameter will increase as $1/\cos(\alpha)$ in the direction of the tilt, but the diameter can remain constant perpendicular to the direction of the tilt. In the case of the cylinders of interest, this tilt (ellipticity) error can be shown by simple geometry to be less than 40 microinches per degree of tilt for small angles.

Of larger consequence is the tilt error due to changes in the specular reflectance angle and the particular geometry of the probe used in the feasibility experiments. This source of error is the major disadvantage of an optical triangulation device that relies on specular light. It can be shown by simple geometry to exceed 8 mils per degree of tilt for small angles for the probe configuration used in the feasibility study. The large magnitude of the error is primarily because the detectors are not oriented perpendicular to the reflected beam. It is therefore extremely important to insert the probe along the axis of the cylinder. Axial alignment to 0.5 millidegree is required to obtain the specified absolute accuracies for the probe used in the feasibility studies. It should also be noted that this error can be eliminated in the case of measuring a true cylinder by adding a rotational degree of freedom to the measurement process. For example, an accurate diameter measurement can be made by rotating the probe or the cylinder on its axis and looking for the minimum

diameter. By adding still another rotational degree of freedom synchronized to the first, elliptical, and multimodal cylinders can also be measured.

Another large source of potential error is due to taper in the bore of the cylinder. Again, for a probe geometry similar to the one used in the feasibility experiments, which is oriented axisymmetric with the cylinder, the error is relatively large (4 mils/degree or 2 mils from one end of the cylinder to the other for a 1-degree full-width taper). Thus,the taper in the cylinders of interest can vary no more than about 2.5 microinches to maintain the required 5 microinch tolerance limit. However, it is worth noting that the measurement degeneracy can again be mitigated by adding another degree of freedom to the measurement system. In this case, translation through the bore is required.

The last source of geometrical error considered is concentricity or displacement error when the probe is not coaxial with the cylinder to be measured. The primary strength of the probe configuration chosen for the feasibility demonstration is that displacement error can be effectively eliminated. After calibration, the probe will measure the true diameter of the bore across any arbitrary axis subject to the constraints mentioned above. If two orthogonal axes are measured simultaneously, then a unique diameter can be determined for any true cylinder. Again, an elliptical or multimodal cylinder will require a rotational degree of freedom to remove the measurement degeneracy.

Although the geometrical error is relatively large, it can be kept within tolerance limits by a judicious choice of probe geometry and measurement fixturing.

Temperature Error

The thermal expansion coefficient of the pyroceram material used in the parts to be measured is on the order of 30 microinches/inch/K at room temperature. The measurement must be performed in an environment controlled to better than 1°C to obtain measurement accuracies in the required 5 microinch range. Good measurement practice dictates actual temperature control approximately one order of magnitude greater than this minimum requirement. In practice, this implies that the measurements must be done isolated from varying or moving heat sources such as found with human proximity.

In the ideal case, the measurement probe would be constructed of ultra-low expansion (ULE) coefficient materials and designed in such a way as to minimize geometrical error due to thermal expansion of the probe body. ULE glasses (30 ppb) are available from Corning Glass and were used in the feasibility experiments described below.

PROBE DESIGN AND FABRICATION

General Probe Layout

Figure 4 shows the detailed assembly drawing of the probe used in the feasibility study. The design takes advantage of commercially available fiber-optic light source components to provide the required collimated illumination beams. It also uses commercial lateral-effect photodiodes mounted to a special thermally stable glass substrate to detect the displacement of the specularly reflected light beams. The probe is designed with two sets of opposing detectors that are used to gauge the surface at four places 90 degrees apart. Due to experimental limitations, only one set of opposing detectors was used at a time for the feasibility experiments.

For the sake of expediency during the feasibility experiments, the four-faceted mirror was mounted via a steel dowel pin to the glass substrate as shown in the diagram. This steel rod represents the largest contributor of thermal error for the feasibility experiments. A 1°F temperature drift causes a 7-microinch error. Alternate designs for the final probe will eliminate this high thermal expansion connection.

In the final design the probe body will be mechanically protected by a cylindrical low-thermal-expansion cover with the mirror attached to the cover. Windows will allow the laser beams to exit and enter the probe body. Again, for the sake of expediency in the feasibility experiments, the probe body was left exposed and the detectors unprotected.

Another compromise made for the sake of expediency in the feasibility design was the selection of the incident angle for the source onto the wall of the cylinder bore. An angle of 30 degrees with respect to the wall was chosen. This shallow angle is undesirable from the point of view of adding error to the measurement (and unnecessary sensitivity via the additional mechanical advantage). The angle selection was necessary, however, to accommodate the oversized geometry of the detectors, as they were the only ones available for the feasibility experiments at the onset of the program. Since that time, new detectors have been located that will allow the angle to be increased to more than 45 degrees.

The glass substrate comprising the exposed probe body with the mirror attached was epoxied to a printed circuit board to supply a rigid disconnectable ground plane. The ground plane board was then mounted to twin preamplifier boards, which were in turn connected to a precision translation assembly. The assembled configuration is illustrated in the photograph in Figure 5.

Probe Body

A close-up photograph of a typical probe body with the detectors mounted is shown in Figure 6. Three of these probe bodies using two different designs were constructed for the feasibility experiments. The more desirable four-hole substrate (see Figure 7),which was designed to hold the four 1.0-mm-diameter GRIN lenses in a precise orientation, was incorrectly masked during the detector mounting process and therefore not available for the feasibility experiments. One of the single-hole substrates (see Figure 8), which was designed to be fitted with two GRIN lenses separated by the mirror support pin and held in place by two spacer pins, was used to collect the data presented below.
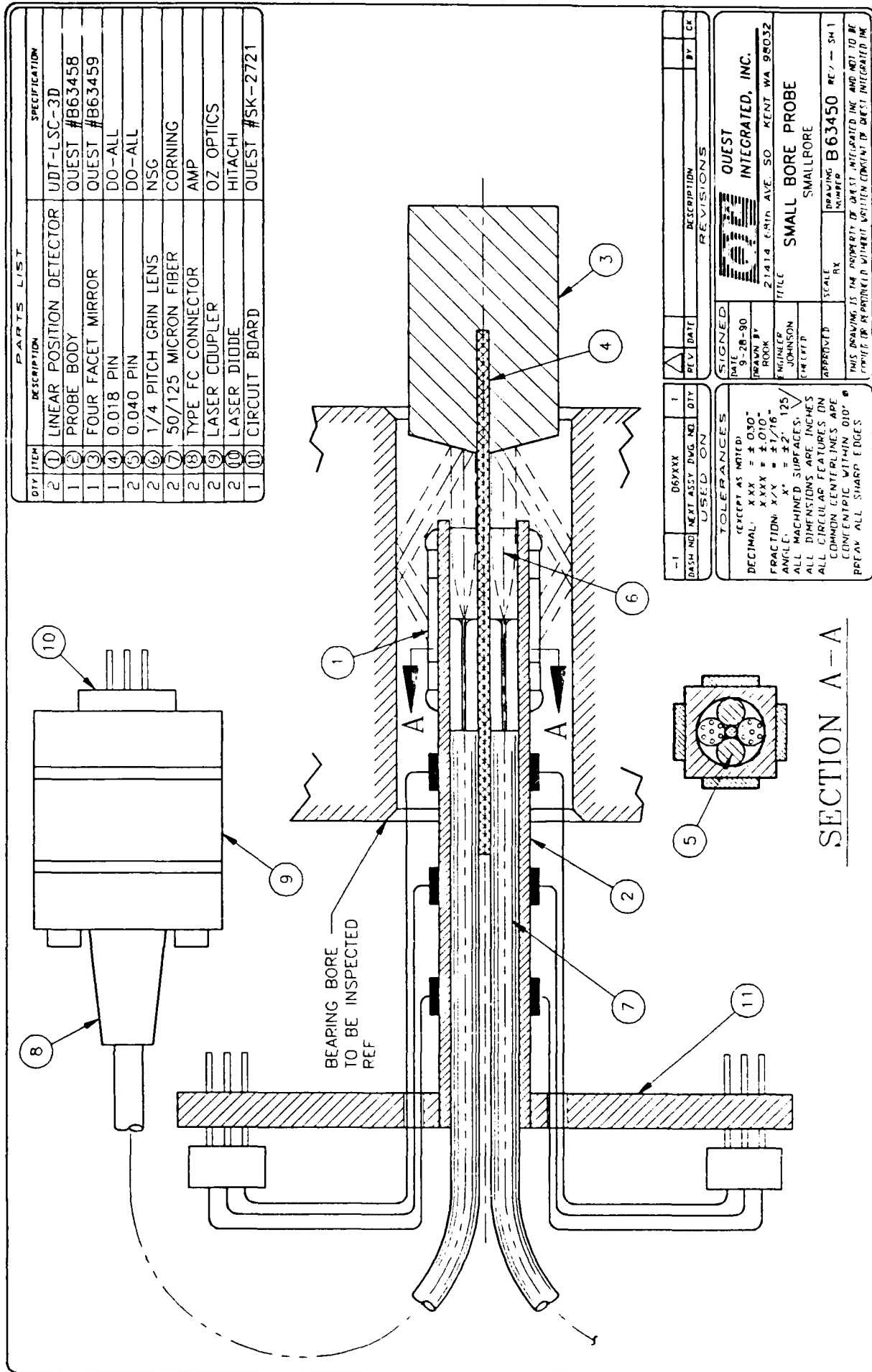
PARTS LIST

QTY	ITEM	DESCRIPTION	SPECIFICATION
2	1	LINEAR POSITION DETECTOR	UDT-LSC-3D
1	2	PROBE BODY	QUEST #B63458
1	3	FOUR FACET MIRROR	QUEST #B63459
1	4	0.018 PIN	DO-ALL
2	5	0.040 PIN	DO-ALL
2	6	1/4 PITCH GRIN LENS	NSG
2	7	50/125 MICRON FIBER	CORNING
2	8	TYPE FC CONNECTOR	AMP
2	9	LASER COUPLER	OZ OPTICS
2	10	LASER DIODE	HITACHI
1	11	CIRCUIT BOARD	QUEST #SK-2721

BEARING BORE
TO BE INSPECTED
REF

SECTION A-A

QUEST INTEGRATED, INC.
21414 64th AVE. SO KENT WA 98032

TITLE SMALL BORE PROBE
SMALLBORE

DRAWING NUMBER B63450 REV — SH 1

TOLERANCES
(EXCEPT AS NOTED)
DECIMAL: X.XX = ± 0.30
X.XXX = ± .010
FRACTION: X.X = ± 1/16
ANGLE: X° = ± 2° .125
ALL MACHINED SURFACES
ALL DIMENSIONS ARE INCHES
ALL CIRCULAR FEATURES ON
COMMON CENTERLINES ARE
CONCENTRIC WITHIN .010
BREAK ALL SHARP EDGES

SIGNED
DATE 9-28-90
DRAWN BY ROOK
ENGINEER JOHNSON
CHECKED
APPROVED

REVISIONS

Figure 4. Small Bore Probe Assembly Drawing
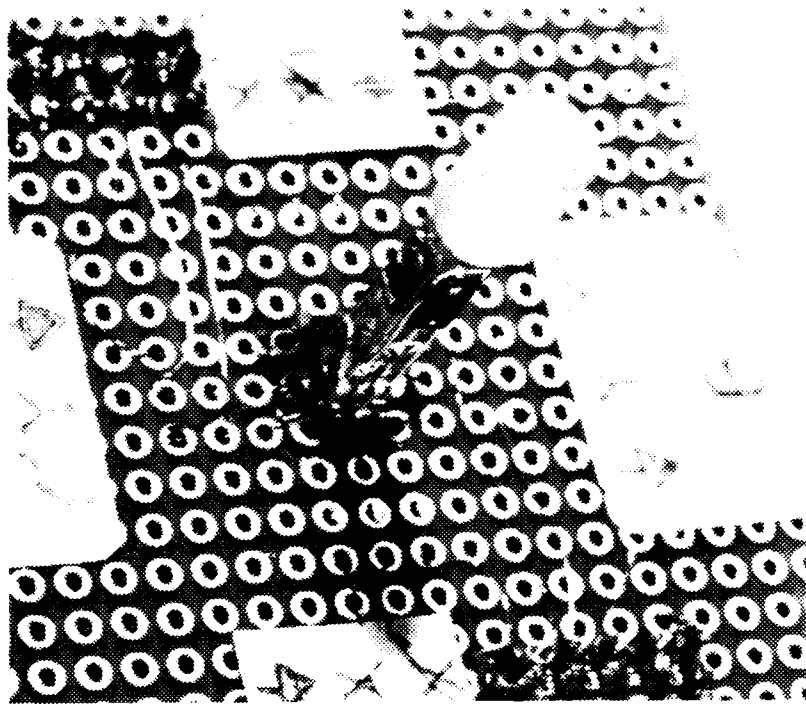
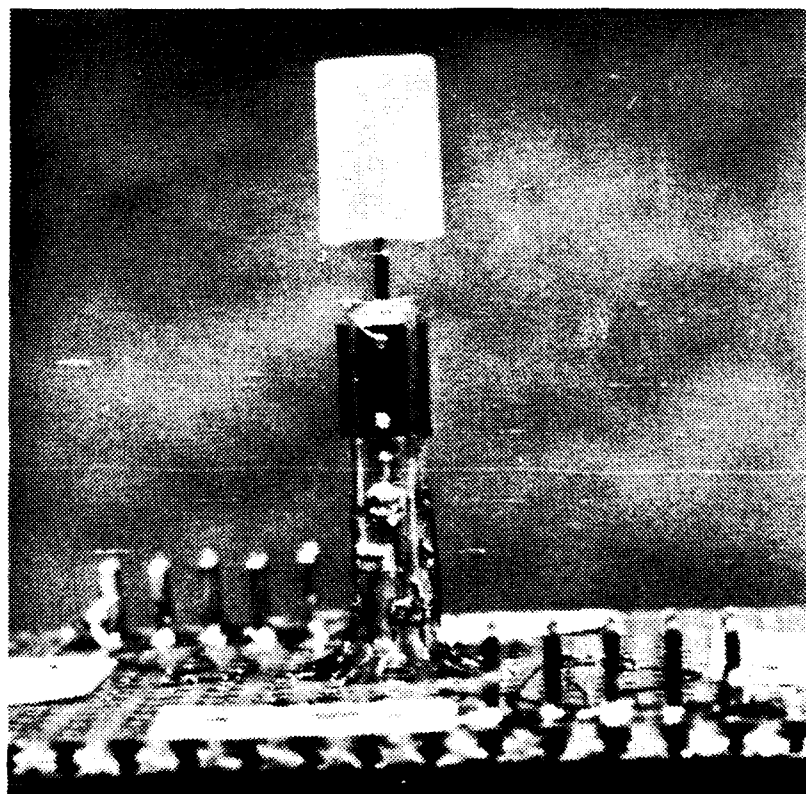Figure 5. Final Experimental Assembly

Figure 6. Probe Body Detail
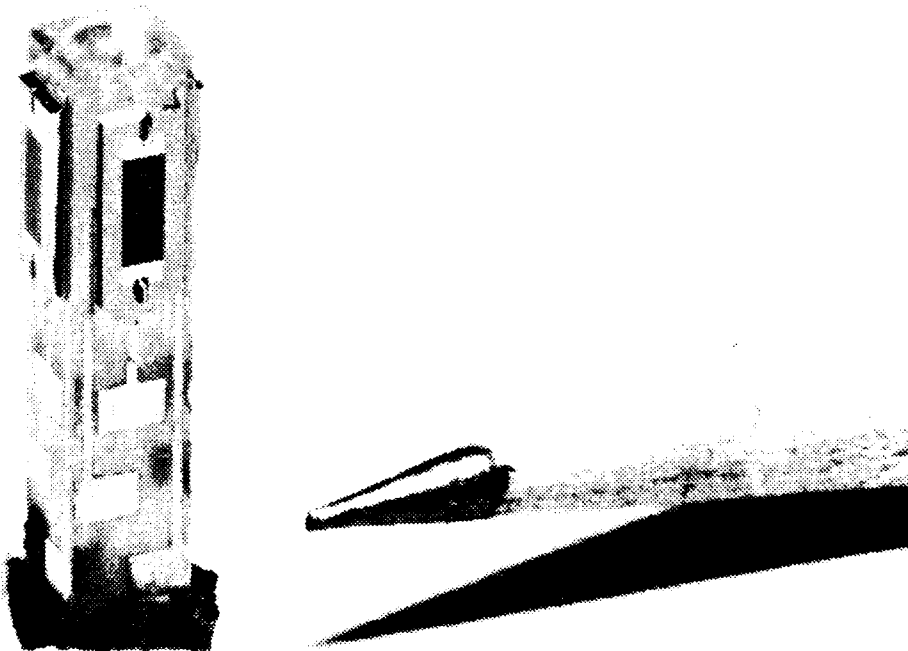
Figure 7. Four-Hole Probe Body

Figure 8. Single-Hole Probe Body

The substrates used for the probe body were abrasive-waterjet (AWJ) machined and drilled at Quest from ULE coefficient glass. This high titanium glass supplied by Corning Glass has a thermal expansion coefficient of approximately 30 ppb per degree Fahrenheit at room temperature. The substrates were AWJ cut to 0.130-inch square blocks 0.875-inch long. They were then AWJ drilled. With a few days of experimentation, the two one-hole substrates were drilled without damage to a hole diameter of 0.098 inch with less than 0.001 inch of taper over the entire length of the hole. The four-hole substrate proved more difficult to machine without taper. The final holes had a uniform diameter of 0.040 inch to a depth of approximately 0.6 inch followed by a taper to approximately 0.020 inch in diameter. Coincidentally, this tapered undersized hole diameter is ideally suited for mounting standard 0.5-mm-diameter GRIN lenses, a feature that was not explored in this feasibility study due to the lead time required for acquisition of the 0.25 pitch lenses.

The substrates were then sent to a hybrid circuit manufacturer (Pacific Hybrids, Beaverton, OR) where the 0.005-inch-wide conductive traces with solder pads were laid on each of the four sides of the substrate. The detectors were then mounted and wire-bonded to the traces before returning to Quest for final assembly and testing. Unfortunately, during shipment many of the delicate wire-bonds connecting the two ends of each detector to the substrate conductors on the unprotected substrates were broken. Attempts at reconnection with silver conductive epoxy and #30 magnet wire were met with enough success to continue the experiment.

Optical Source

As mentioned previously, each of the light sources consisted of a diode laser coupled to a fiber optic and terminated by a collimating GRIN lens. This assembly produced a stable, high-intensity, collimated light beam with a diameter somewhat less than 1 mm.

Lasers/Drivers

The 20-mW laser diodes (Hitachi 6705A) used were index guided and operated at 780 nm. The diodes were mounted to a commercially available fiber-optic coupler made by Oz Optics. This coupler uses a pair of GRIN lenses and a tilting mount to launch light from the laser into the fiber with an efficiency exceeding 90%. The mechanical coupling provided on the output side of the coupler is a type FC fiber-optic bayonet/screw mount, which is suitable for mating to a standard AMP FC-944 terminated cable assembly. The photograph in Figure 9 shows the assembly with the fiber attached.
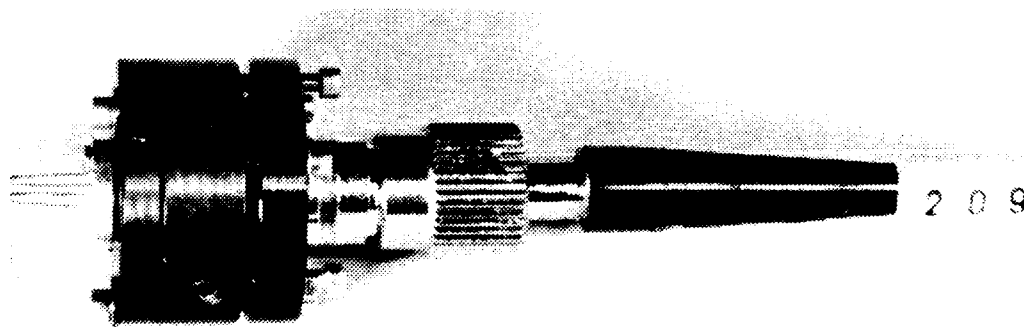

Figure 9. Diode Laser Assembly

The lasers were powered by Sharp IC3C02 laser drivers. These current drivers are feed-back stabilized via the back-faceted diode on the laser package to provide a constant optical power output to approximately one part in a thousand, which is sufficient for the feasibility study.

Fiber Optics

The multimode optical fiber used had a 50-micron core diameter with a 125-micron cladding diameter surrounded by a 900-micron polyethylene jacket.

GRIN Lenses

The 1.00-mm-diameter, 0.25-pitch collimating GRIN lenses (Nippon Sheet Glass) were bonded to ends of the fiber using a UV curable epoxy (Norland #68). Alignment of the fiber was accomplished using a specially made jig employing a five-axis micromanipulator to position the lens relative to the fiber. The resulting GRIN\fiber connection proved easy to make, highly efficient, and very durable. A photograph of a typical assembly is shown in Figure 10.
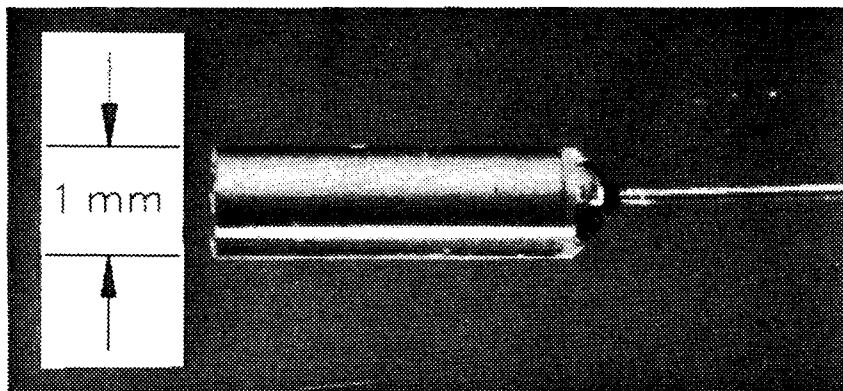
Figure 10. GRIN to Fiber Assembly

Faceted Mirror

The first surface four-faceted mirror was made from ULE glass and aluminized. The facets were fabricated at 15 degrees to the mirror's axis. The facets were ground flat to three waves and coated with pure aluminum. A shallow 0.020-inch hole was drilled at the apex of the four facets to provide a mounting locator for the mirror support pin. The steel support pin was then fastened to the mirror using a thermal-set epoxy resin prior to final assembly in the detector substrate. A detail of the faceted mirror assembly is shown in Figure 11.

Linear Position Detectors

The linear position detectors, which were unmounted, were purchased from United Detector Technology (PIN-SL3). The detectors were then mounted as described above. Details of the detector masking configuration on the substrate are shown in Figure 12. Subsequent to mounting, detectors with a superior geometric configuration and electrical specifications were located (Hamamatsu S3272), but program constraints did not allow testing of these detectors during the initial feasibility study.
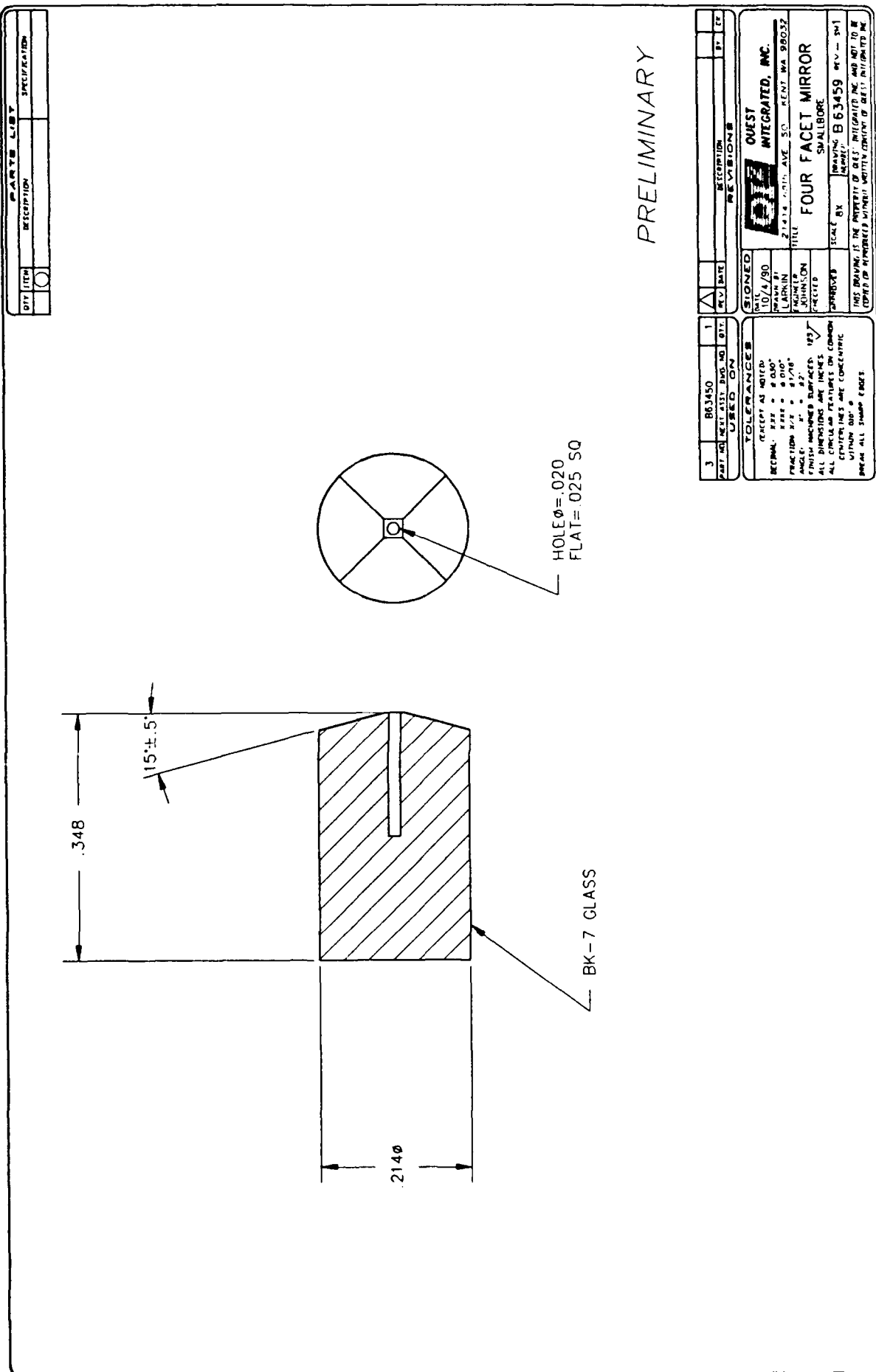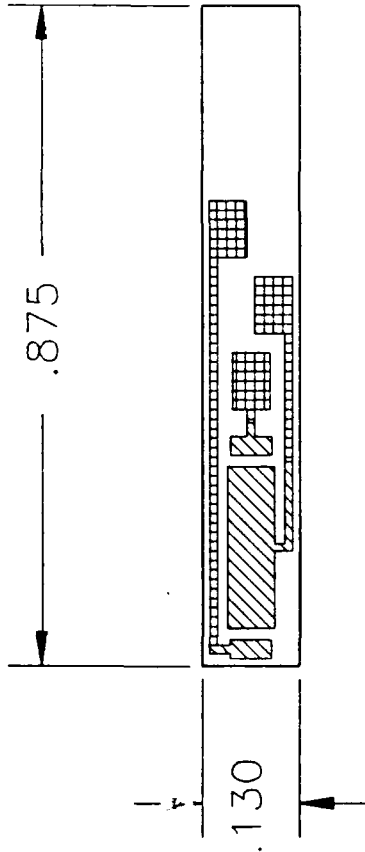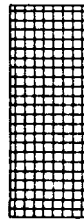
Figure 11. Faceted Mirror Detail

NOTES:
DEPOSIT ON 4 SIDES
OF BLOCK

.875

.130

SCALE: 4X

AU PRINT

PD/AG PRINT

PRELIMINARY

REVISIONS
REV DATE DESCRIPTION BY CK

USED ON
DASH NO NEXT ASSY DWG NO QTY
-1 D6XXXX 1

TOLERANCES
(EXCEPT AS NOTED)
DECIMAL: X.XX = ± .030"
X.XXX = ± .010"
FRACTION X/X = ± 1/16"
ANGLE: X° = ±2° 125/
ALL MACHINED SURFACES
ALL DIMENSIONS ARE INCHES
ALL CIRCULAR FEATURES ON
COMMON CENTERLINES ARE
CONCENTRIC WITHIN DIA
BREAK ALL SHARP EDGES

SIGNED
DATE 10-11-90
DRAWN BY ROOK
ENGINEER R JOHNSON
CHECKED
APPROVED

QUEST
INTEGRATED, INC.

21414 68th AVE SO. KENT WA 98032

TITLE SMALL BORE TRACE PATTERN
SMALL BORE

DRAWING NUMBER A 63474 REV – SH 1

SCALE 4X

Figure 12. Small Bore Trace Pattern

Preamplifier Electronics

The preamplifier electronics shown schematically in Figure 13 were designed to be both low in noise and versatile, allowing for both AC and DC operation. Only DC operation was used in the feasibility experiments.

Data Acquisition System

The data acquisition system consisted of a PC and an eight-channel 12-bit analog-digital converter. The A/D was operated in differential mode to monitor two opposing detectors simultaneously. The signals from each side of the two linear position detectors were thus digitized prior to performing the necessary arithmetic with the computer. The laser power and the gains of the preamplifiers were adjusted to take maximum advantage of the full dynamic range of the A/D over a 0.010-inch measurement range for the probe. With this arrangement, the switching resolution of the digitizer limits the resolution in the diameter measurement to approximately one part in four thousand for each input channel or 5 microinches in the calculated distance value in the optimum situation (perfect linearity and identical sensitivities for both detectors). In practice, as shown below, the resolution of measurement was limited to approximately 8 microinches. Additional measurement resolution will require a higher resolution A/D.

To provide data on noise, stability, and repeatability, the software was designed to perform a series of 100 sequential measurements at 0.1-second intervals, to calculate the normalized difference signal for each data point, and to perform a statistical analysis on the data sample to yield the average and standard deviations for the measurement. The raw data were displayed in real time in A/D counts for operator monitoring, and the statistical data were presented after each measurement sequence was completed. The resulting data were fed into a standard spreadsheet program for further analysis.

Experimental Arrangement

The experimental apparatus was assembled as shown in the photograph in Figure 14. For the calibration and stability measurements, the probe assembly was positioned between the faces of a precision caliper micrometer as shown. The caliper diameter was adjusted to yield signals that were optimum for digitization (approximately 0.2470 inch for the feasibility experiment device tested). The appropriate measurements were made by translating the caliper relative to the probe using a precision computer-controlled translation stage.

No special account was taken of the thermal environment for these feasibility experiments. However, the apparatus was placed in a cardboard enclosure to suppress thermal transients that would affect the short-term diameter measurements.
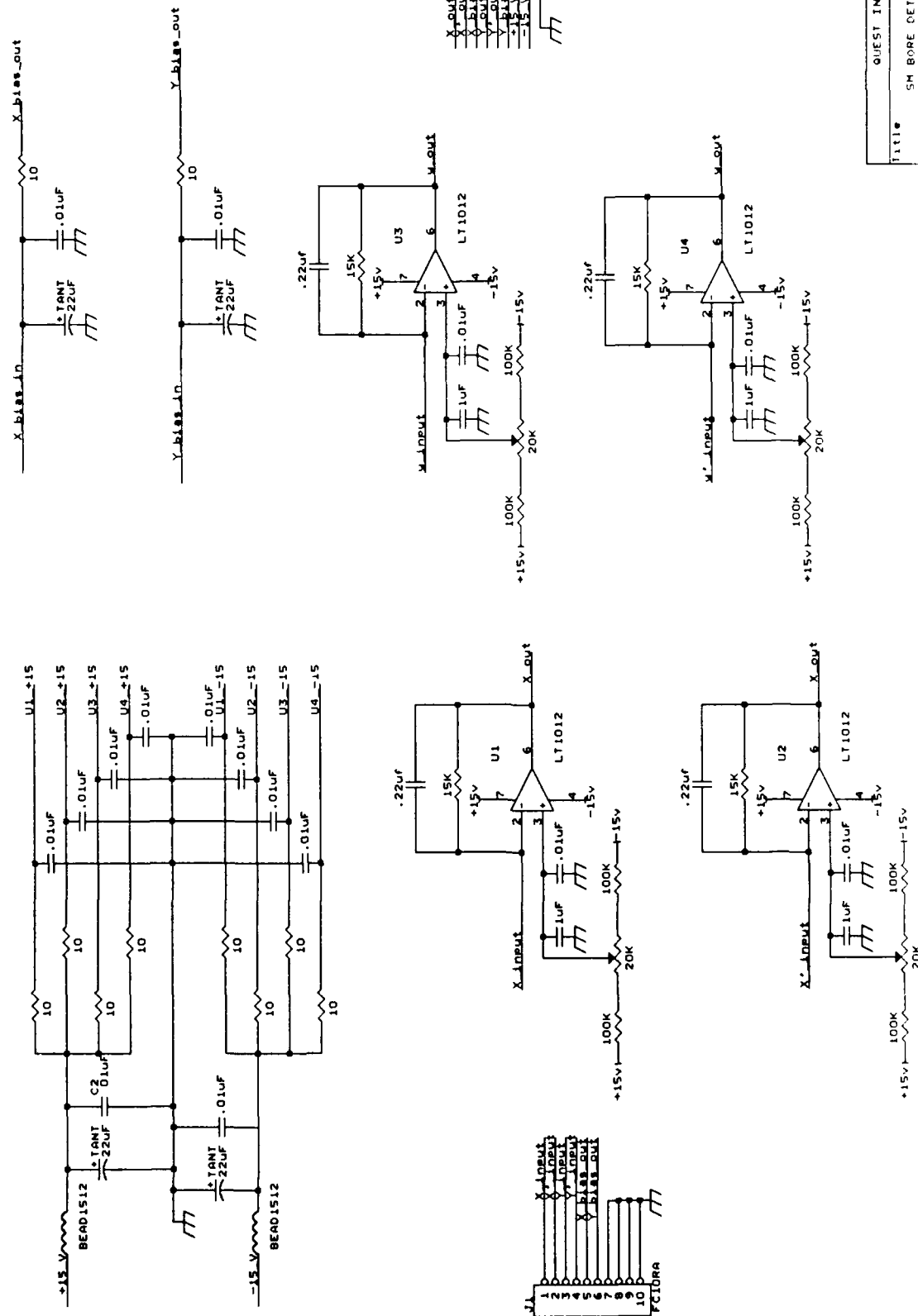
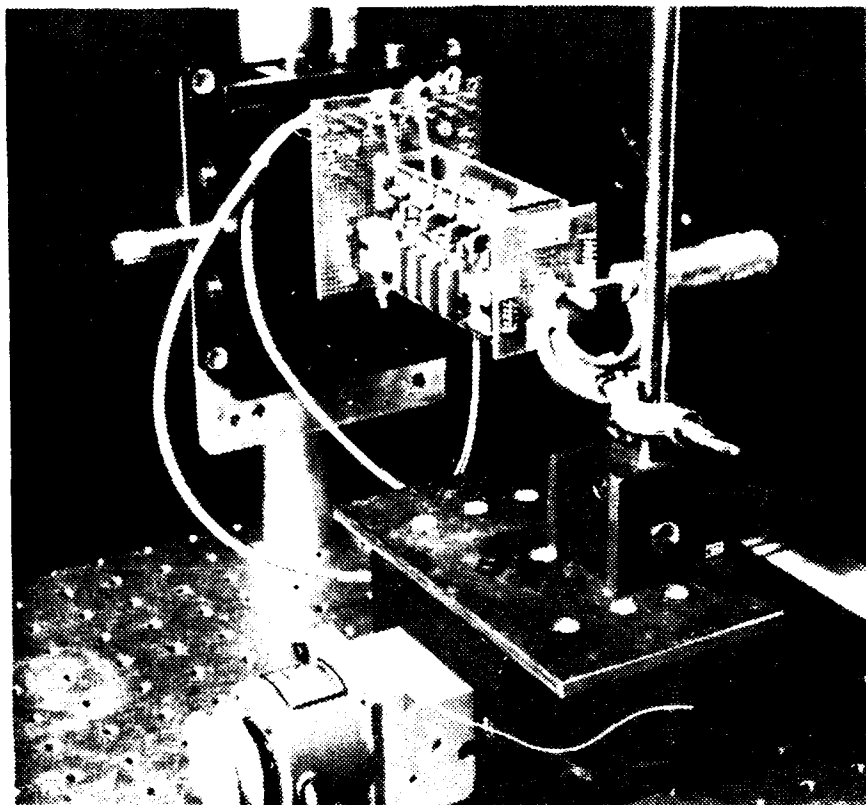Figure 13. Preamplifier Schematic

Figure 14. Experimental Apparatus

VERIFICATION EXPERIMENTS

Calibration Range and Linearity

Calibration of the individual detectors is straightforward. A planar specular surface is placed at a known distance from, and exactly parallel to, the axis of the probe. The normalized difference signal is then recorded as a function of this radius value. In the feasibility experiments, two opposing detectors were calibrated simultaneously by placing the probe between the faces of a precision caliper micrometer and translating the micrometer perpendicular to the axis of the probe. By keeping the diameter of the caliper constant (except for variations due to thermal fluctuations), it is often possible to distinguish errors in the translation stage from detector/amplifier errors.

To obtain maximum linearity and resolution in the ideal case, both detectors were arranged so that the centroid of the specularly reflected beam illuminated the electrical center of the detector at the nominal diameter of the measurement, 0.2500 inch for the actual bores of interest. In the feasibility experiments, the optimum diameter was 0.2470 inch for the probe used. The caliper diameter was adjusted accordingly for the first calibration.

The results of the first calibration are shown in Figure 15 below. Plotted is the normalized difference output signal versus the displacement (in 0.001-inch increments) from the optimum radius value for each of the two detectors. Both curves show that the 0.001-inch increments are easy to distinguish. The curve for detector B is nearly linear over the full dynamic range of the calibration measurement (0.010 inch), as expected. The curve for detector A, while monotonic, has a quadratic shape. This may be due to the relatively high contact resistance of the repaired detector wire bonds, a problem that should be eliminated in future attachment schemes.
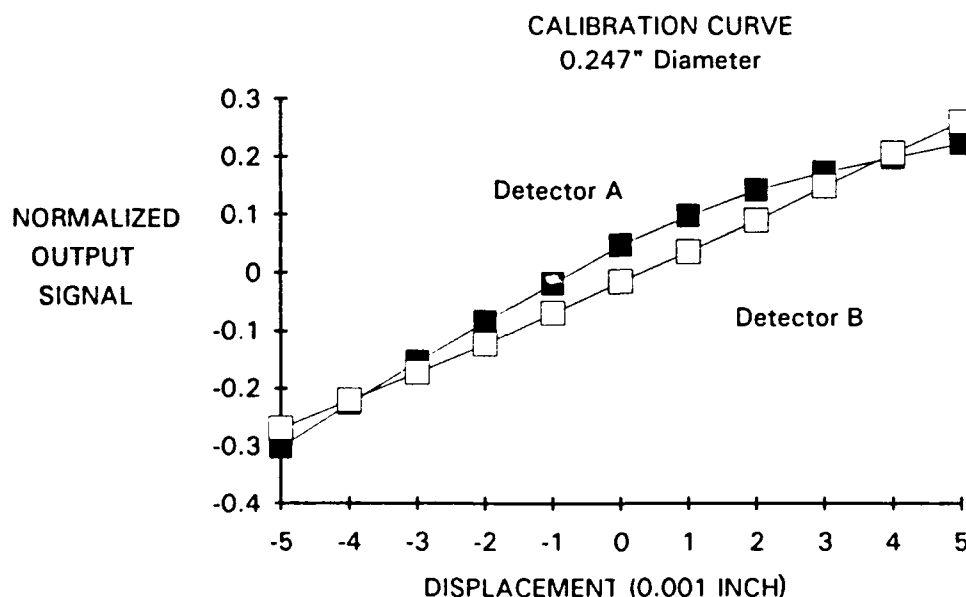

Figure 15. Experimental Calibration of Detectors

If each detector response (normalized difference signal) is linear and has the same slope, then in the easiest case (no tilt or wedge) the diameter measurement is simply a matter of adding the two normalized difference signals and applying the calibration scale factor. Since the detector response function remains relatively stable for a specified temperature, a periodic check on a reference diameter will ensure the accuracy of the measurement over the full measurement range of the probe. In the real world, however, nothing can be relied upon to be that simple, and a computer-assisted look-up table or function generator will likely be used to translate the output signals to real diameters.

Experimental Measurement Resolution

To get a handle on the measurement resolution of the feasibility probe, an attempt was made to generate a calibration curve using smaller, higher-resolution steps. The precision translation stages immediately available touted repeatable linearity and resolution of 8.0 microinches. Figures 16 and 17 show the calibration curves for the same probe as above taken with 0.00020 inch steps using this translation stage. In the first run, the caliper micrometer was set to approximately 0.245 inch. In the second run, the caliper micrometer was changed to 0.246 inch to look for systematic translation (versus measurement) error.

Aside from the sensitivity roll-off in detector A, a periodic structure in the 50 to 100 microinch amplitude range can be clearly seen in both of these high-resolution calibration curves. Figure 18 is an expanded plot of the data from Figure 17 displayed as the difference between successive measurements. The results from both detectors are shown as they appear to the observer watching the caliper micrometer translated perpendicular to the probe axis at a constant diameter. As a consequence, detector A is shown as a positive displacement per step and detector B is shown as a negative displacement per step.
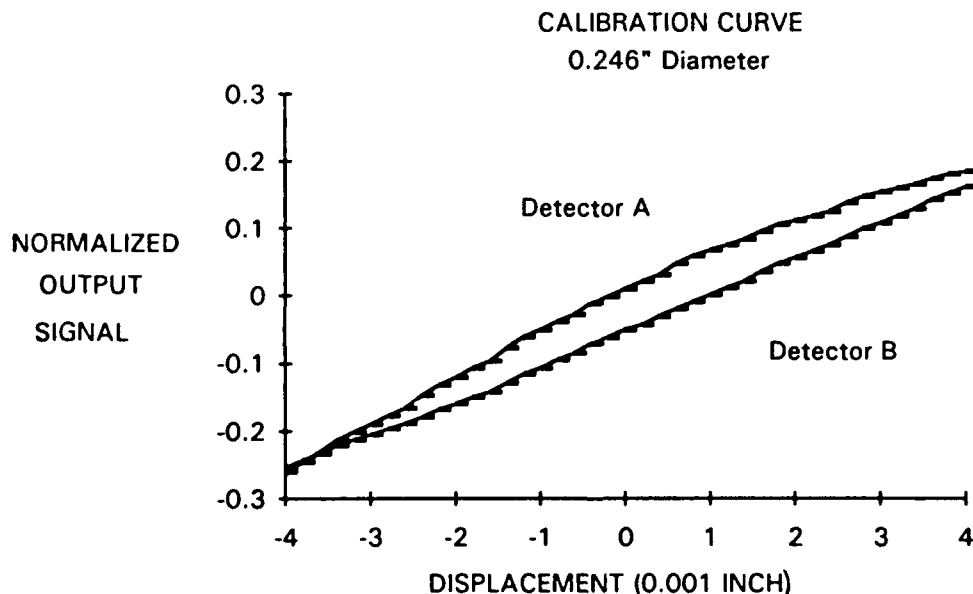

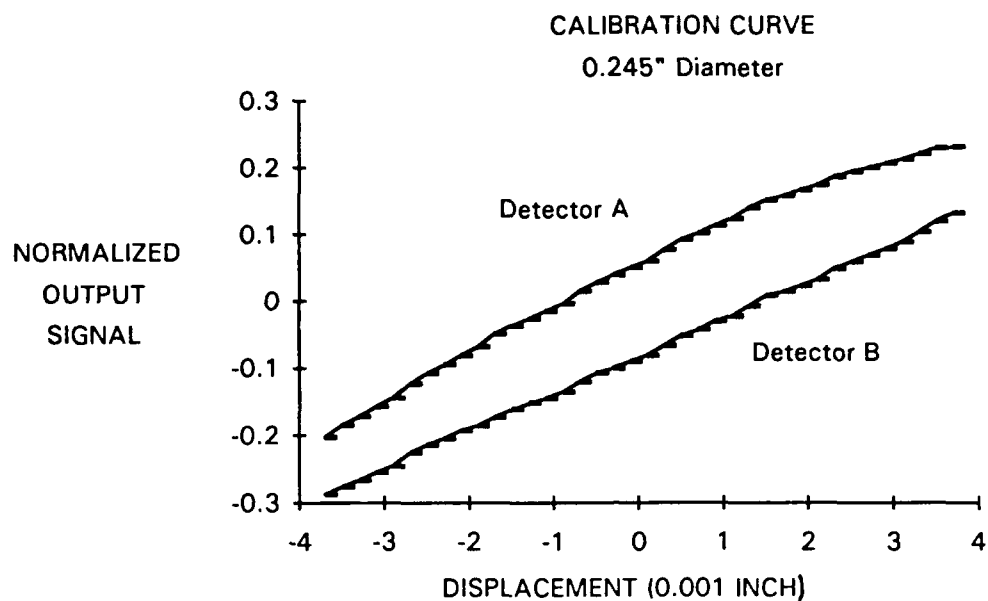Figure 16. Experimental High-Resolution Calibration Curves, Run 1

CALIBRATION CURVE

0.245" Diameter

Figure 17. Experimental High-Resolution Calibration Curves, Run 2
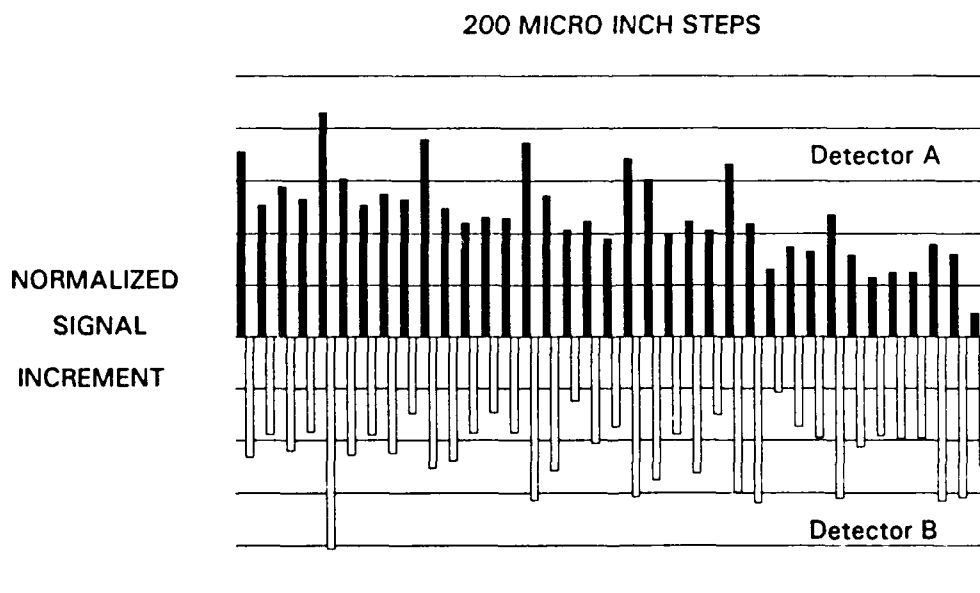
200 MICRO INCH STEPS

Figure 18. Detector Signal Change per Translation Stage Increment

The conclusion drawn from the above plot is that the translation stage, contrary to manufacturers' literature, does not move in uniform step sizes. In fact, there appears to be a harmonic in the screw thread that results in a periodic component to the translation linearity approximately every 0.001 inch. Therefore, this stage cannot be used for the fine-step checking as originally hoped.

As an interim measure, a flat-faced piezoelectric translator with a full dynamic range of 10 microinches was employed to verify that the measurement resolution achievable was at least equivalent to the switching resolution achievable with the 12-bit A/D converters being used for the feasibility experiments. The experiment confirmed that an 8-microinch step was easily detectable at several discrete radii.

As can be seen from the above charts, the experimental sensitivity of the feasibility experiments is approximately 55 millivolts/mil or equivalently 55 microvolts/microinch. Thus, even 1-microinch-resolution goals are well above the expected rms detector/amplifier noise floor of 7 microvolts. Barring some type of unforeseen position granularity on the detector, measurement sensitivities in the 0.5 microinch range should be possible. Unfortunately, this assumption could not be verified during the feasibility experiments for lack of an appropriate translation platform and a high enough resolution A/D. The fixturing and A/D conversion must be refined in the next phase of work.

Repeatability and Stability of the Measurement

Several repeatability and stability experiments were performed during the feasibility study. Figure 19 is typical of the results. In successive measurements separated by approximately one minute, the caliper micrometer was measured by the probe. The resultant values are plotted as the difference from the mean value of the group of measurements in the figure. The error bars represent the switching resolution of the A/D converter. The apparent super-resolution of each of the measurements is due to the statistical measurement procedure mentioned above where each reported measurement is an average of one hundred individual measurements as described previously.

Figure 19 shows a scatter in the measurement slightly larger than that expected from the noise in the least significant bit of the A/D. In physical units, the measurements remained stable and repeatable to within 16 microinches. Some of the long-term variations (up to 10 microinches) in this series of measurements can likely be attributed to the thermal drift in the caliper, the interim probe design, and the fixturing, since no attempt was made to control the thermal environment. The more random jumps may be attributable to mode hopping in the laser/source configuration used, a problem that will be rectified in the next phase of work.
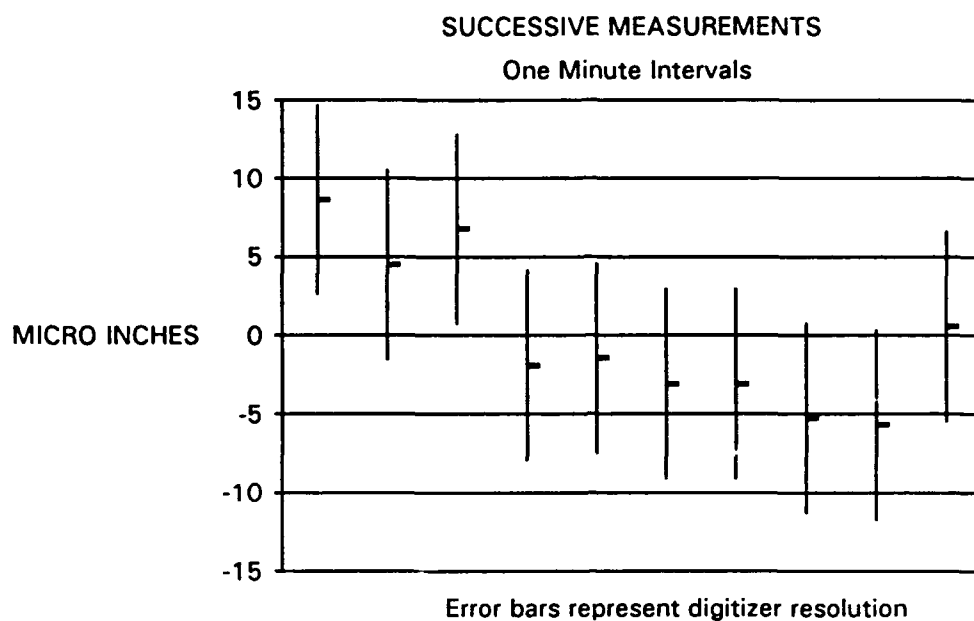
SUCCESSIVE MEASUREMENTS

One Minute Intervals

Error bars represent digitizer resolution

Figure 19. Measurement Drift Versus Time

CONCLUSIONS AND RECOMMENDATIONS

Phase I Feasibility Study Conclusions

The Phase I feasibility study showed that optical triangulation profilometry can be successfully adapted to the measurement of small-diameter bores. The accuracies demonstrated in the feasibility experiments exceeded 20 microinches. A fundamental error analysis showed that the accuracies can be extended to better than 1 microinch with minor changes in the probe design and digitizer resolution. Based on the experimental results of the feasibility study, it is easy to visualize a commercial version of this probe that will have the advantages of relatively low cost, high accuracy, and ease of use and that will meet not only the measurement needs of the Air Force gyro bearing program, but also a wide range of precision commercial applications.

Phase II Design Recommendations

In the next phase of development, several design improvements are suggested to improve the performance, ruggedness, and cost effectiveness of the small bore probe. These are described briefly below.
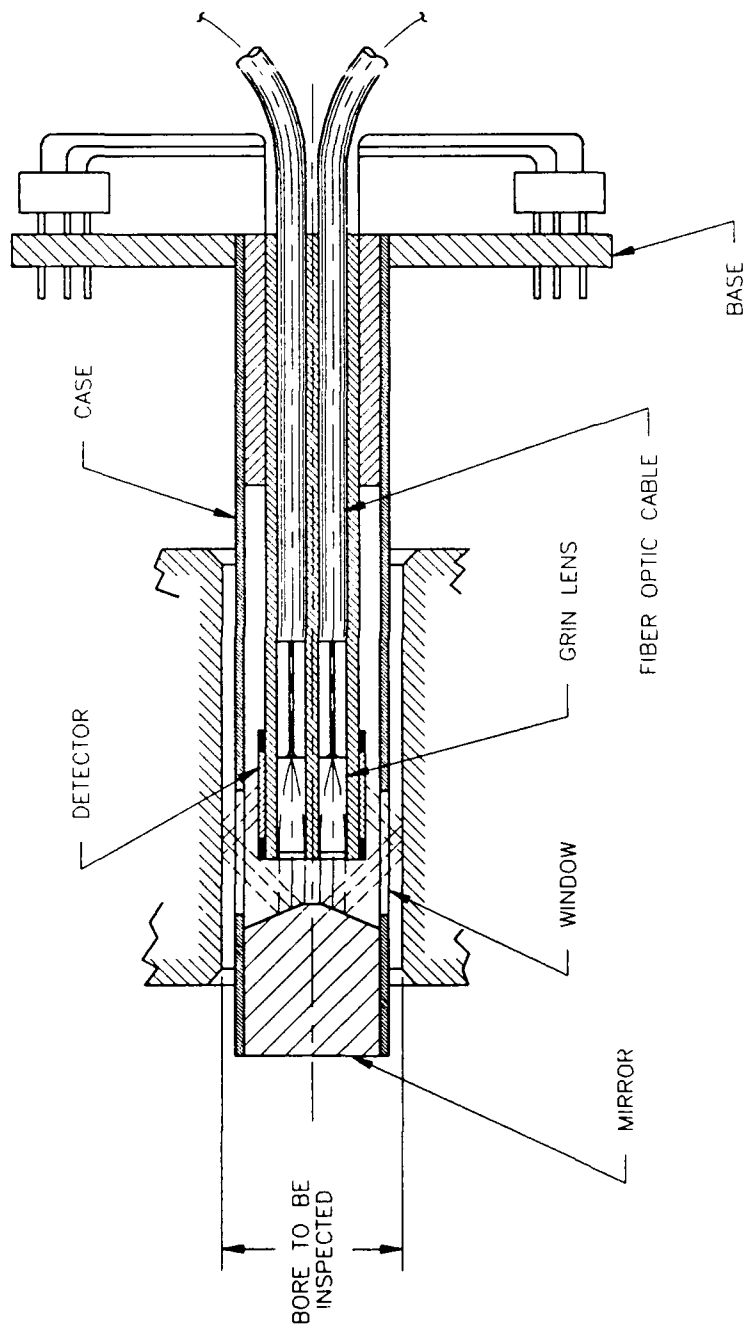
Probe Design

To increase the thermal and mechanical stability of the optical components, it is recommended that all the components used in the probe head be constructed from ULE glass. The concept outlined in Figure 20 will assure a rigid optical path with high thermal immunity. In the recommended design, the substrate that holds the detectors and the GRIN lenses is connected to the four-faceted mirror via an external, windowed support tube. The tube provides mechanical protection for the delicate detector bonds and keeps the mirror in a fixed position with respect to the detectors with minimal thermal expansion effects. A four-hole design is recommended for the probe substrate. This design will simplify the assembly and alignment of the optics, and it will assure greater mechanical stability for the optical path.

The use of 0.5-mm quarter-pitch GRIN lenses is recommended rather than the 1.0-mm lenses used in the feasibility experiments. These smaller lenses will form a smaller-diameter beam, which can be more easily contained on the detectors without complex fixturing during initial alignment of the optical path.

Short single-mode fibers are recommended to replace the long multimode fibers used in the feasibility experiments. If these fibers are mounted in a semirigid environment, then position noise due to of the fiber and mode hopping should be eliminated. It is desirable that source lasers be mounted as close as possible to the probe body to facilitate a compact package for the entire active portion of the probe.

Mounting of the preamplifiers in close proximity to the detectors with adequate ground plane shielding is recommended to reduce the effects of EMI pickup. The annoying presence of nearby radio stations in ground loop problems was an issue in the feasibility experiments.

Figure 20. Probe Body Design

Support Electronics and Software

One of the principal difficulties with the feasibility experiments was the lack of digitizer resolution, which prevented demonstration of the theoretical sub-microinch resolution capabilities of the system. The use of a 16-bit A/D converter is recommended to replace the 12-bit converter used in the feasibility tests.

Simultaneous eight-channel data acquisition is recommended in order to measure two diameters simultaneously. Only four channels (one diameter) were used in the feasibility experiments. Simultaneous measurements are required to reduce repeatability error due to transient mechanical instabilities in the probe and the fixturing for the measurement.

The recommended electronics package is relatively simple. A block diagram of the system is shown in Figure 21. The detectors drive low-noise preamps as in the feasibility experiment. Each detector channel is digitized and read by an internal CPU along with the encoder positions for the translational and rotational degrees of freedom and the local temperatures.

The system software should compute the normalized difference signal in real time and translate the signals to displacement values via look-up tables. The translational and rotational degrees of freedom should also be monitored and the geometrical correction factors calculated by the CPU in real time. The true temperature-compensated diameter, circularity, taper, and cylindricity should be displayed at the completion of the measurement sequence. Display options should include either fixed format numbers or a graphical format depending upon customer requirements and cost considerations.

It is recommended that the software support package also include automatic setup and calibration, automatic measurement sequencing and data acquisition, and extensive internal error checking with periodic absolute reference checking. Foremost, the software should provide a simple, easy-to-use operator interface to the complex measurement process.

Mechanical Configuration

The mechanical fixturing and associated electronic support hardware for the measurement system are illustrated in Figure 22. Precision mechanical fixturing for at least one rotational and one translational degree of freedom as indicated in the figure is recommended. By fixturing the probe precisely on the axis of rotation of the cylindrical bore, the specular reflectance errors, eccentricity errors, and taper errors can be measured and decoupled. Translation along the axis of the bore will allow measurement of and compensation for bore taper.

Potential Applications

While development costs on this precision measurement tool are significant, manufacturing costs are expected to be low. It is also likely that heads for different diameters will be interchangeable, which would further reduce costs. The significance of being able to obtain microinch-accuracy measurements easily and at moderate costs cannot be ignored. Such a tool will have wide applicability in all forms of tubing and internal bore measurements.
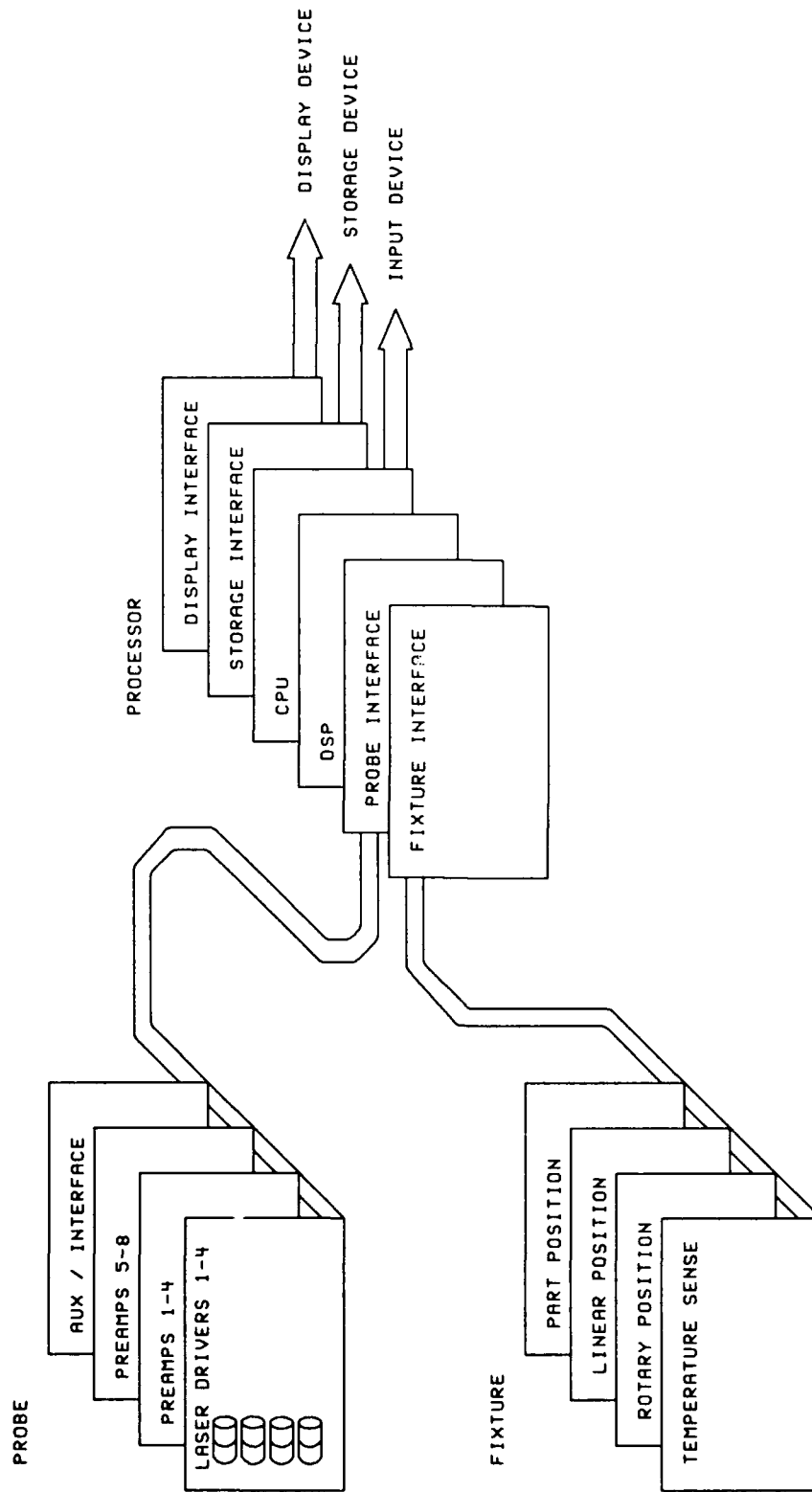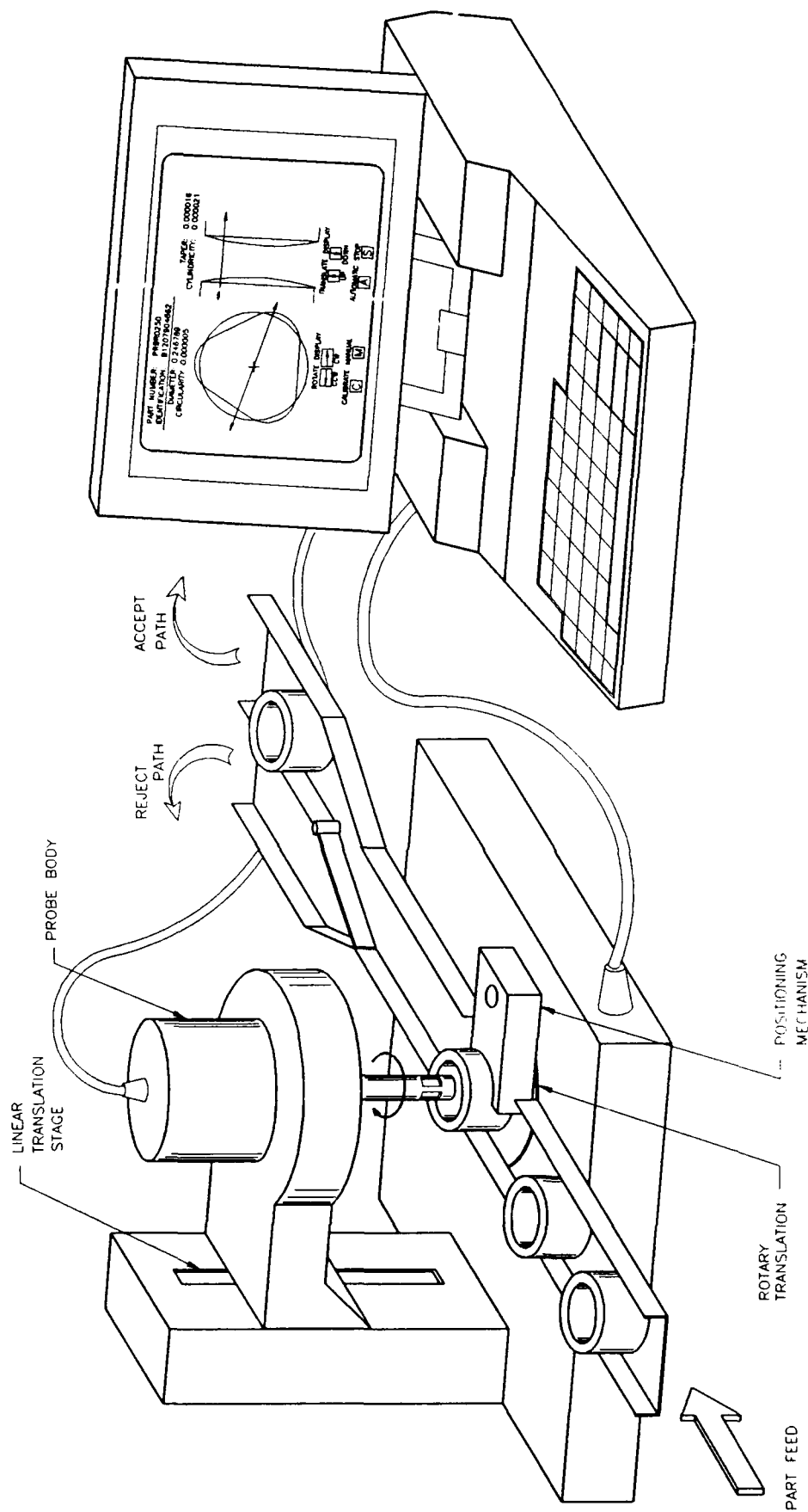
Figure 21. Electronic Signal Processing Block Diagram

Figure 22. Small Bore Gauge Instrument Configuration

DISTRIBUTION LIST

Addressee	No. Copies
BMO/SDD NAFB, CA 92409-6468	2/0
BMO/MYCC NAFB, CA 92409-6468	LTO
BMO/SDC NAFB, CA 92409-6468	2/0
TRW/EDC P.O. Box 1310 San Bernardino, CA 92402	1/0